

Oscillating pendulum decay by emission of vortex rings

Diogo Bolster,¹ Robert E. Hershberger,² and Russell J. Donnelly^{2,*}

¹*Department of Civil Engineering and Geological Sciences, University of Notre Dame, Notre Dame, Indiana, 46556 USA*

²*Department of Physics, University of Oregon, Eugene, Oregon, 97403 USA*

(Received 23 September 2009; revised manuscript received 14 December 2009; published 26 April 2010)

We have studied oscillation of a pendulum in water using spherical bobs. By measuring the loss in potential energy, we estimate the drag coefficient on the sphere and compare to data from liquid-helium experiments. The drag coefficients compare very favorably illustrating the true scaling behavior of this phenomenon. We also studied the decay of amplitude of the pendulum over time. As observed previously, at small amplitudes, the drag on the bob is given by the linear Stokes drag and the decay is exponential. For larger amplitudes, the pendulum bob sheds vortex rings as it reverses direction. The momentum imparted to these vortex rings results in an additional *discrete* drag on the bob. We present experiments and a theoretical estimate of this vortex-ring-induced drag. We analytically derive an estimate for a critical amplitude beyond which vortex ring shedding will occur as well as an estimate of the radius of the ring as a function of amplitude.

DOI: [10.1103/PhysRevE.81.046317](https://doi.org/10.1103/PhysRevE.81.046317)

PACS number(s): 47.10.-g, 47.37.+q

I. INTRODUCTION

The study of pendulum motion is a classical problem in physics and understanding the influence of fluid drag on its decay dates back to Stokes [1]. He derived a simple expression for drag on a sphere at low Reynolds numbers, which was later expanded on to include the effects of added mass and other phenomena (e.g., Landau and Lifshitz [2]).

At low Reynolds numbers, this drag, F_D^s , can be expressed as

$$F_D^s = 6\pi\eta R_s V \left(1 + \frac{R_s}{\delta}\right). \quad (1)$$

At larger Reynolds numbers, it is observed that the drag has an additional component, which is proportional to velocity of the pendulum squared [2]. This drag, F_D^l , can be expressed as

$$F_D^l = C_D V^2 + F_D^s. \quad (2)$$

Here, η is the viscosity, ρ the density, and $\nu = \eta/\rho$ is the kinematic viscosity of the fluid surrounding the sphere whose radius is R_s . $V = \omega A$ is the velocity, A is the amplitude of the oscillation at frequency f , $\omega = 2\pi f$ and $\delta = \sqrt{2\nu/\omega}$ is the thickness of the boundary layer surrounding the sphere. C_D is a drag coefficient, which is typically empirically fit (e.g., Gonzalez and Bol [3] and Alexander and Indelicato [4]). More complex expressions for the drag on a sphere that include acceleration effects can be found (e.g., Mordant and Pinton [5] and Lyotard *et al.* [6]).

We define the Reynolds number as

$$\text{Re} = \frac{2R_s V}{\nu}, \quad (3)$$

The influence of fluid drag has become a topic of great interest to the quantum fluids community, where studies of oscillating objects in superfluid environments have been conducted (for a recent review, see Skrbek and Vinen [7]). In

many of these cases, a transition from a drag that is linearly proportional to the velocity to quadratically proportional is also observed. In many cases, the quadratic drag is associated with vortical and turbulent structures behind the sphere. Additionally, this drag and the interaction of a body with vortical structures plays a crucial role in swimming dynamics where animals oscillate or flap their bodies in such a way as to generate vortices that propel them (see Linden and Turner [8], Dabiri and Gharib [9], von Ellenrieder *et al.* [10], Blondeaux *et al.* [11], and Afanasyev [12]).

Over the past few decades, significant experimental and theoretical researches have been performed on unsteady flow past a sphere. The generation of a vortex ring during the impulsive flow of a sphere at low to moderate Reynolds number was observed experimentally by Taneda [13]. Later Bentwich and Milow [14], Sano [15], and Felderhof [16] provided a theoretical solution to show the *birth* of such a vortex ring. Various numerical studies (e.g., Yun *et al.* [17], Blackburn [18], and Constantinescu and Squires [19]) at small and large Reynolds numbers have observed vortex rings and other vortical structures behind a sphere. Specifically, Yun *et al.* [17] illustrated that a numerical model, which does not capture the vortex rings, will underestimate the actual drag on a body.

In this study, we show that, as expected, at sufficient amplitude, the drag on a spherical pendulum is greater than that predicted by Stokes [1]. We demonstrate experimentally the existence of a regime where a vortex ring is shed at the end of each swing and show that the additional decay on amplitude beyond Stokes [1] can be estimated analytically as the impulse given to these rings. The pendulum system can be characterized by two dimensionless numbers. These are

$$\text{KC} = \frac{\pi A}{R_s} \quad \text{and} \quad \text{St} = \frac{4fR_s^2}{\nu}, \quad (4)$$

which are the Keulegan-Carpenter and Stokes numbers, respectively.

*rjd@uoregon.edu

II. APPARATUS

We operated the pendulum in two ways: with a fixed suspension and with a motor-driven suspension. The fixed suspension was used to observe the decay of the pendulum's amplitude. The driven suspension permits observation of the pendulum motion at constant amplitude near the resonant frequency of the pendulum.

A glass aquarium tank is filled with the fluid in which the pendulum bob oscillates. For the cases described here, the working fluid is de-ionized water, with a small amount of thymol blue dissolved therein. The pendulum is constructed using various spherical metal balls suspended on either light-weight magnet wire or fishing line. A brushless linear motor, driven sinusoidally, was used for the driven suspension.

A digital video camera was used to measure the amplitude of oscillation at any point in time. The ring radii were measured with a digital camera. The camera setups were calibrated by imaging a steel rule located on the focal plane.

In the decaying oscillation experiments, two pendulum lengths were used (315 and 155 cm). Assuming a maximum amplitude of 10 cm, then the angle cosines would be $\cos \theta = 0.9995$ and 0.9979 , thus preserving the small-angle approximation. For most of the observations, the camera location was such to limit the parallax error to less than 0.15%.

The Baker electrolytic technique is used to visualize the vortex rings from the spherical bobs. The electrochemistry and other physical details are described in Mazo *et al.* [20]. The pendulum and resultant rings are photographed in silhouette.

The oscillation amplitude is extracted from the recorded images with the use of an in-house-written software. Vortex ring sizes were measured using standard software packages (such as PHOTOSHOP).

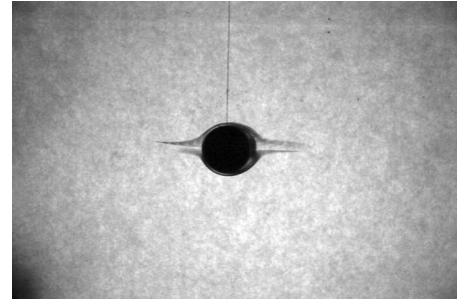
III. DRAG COEFFICIENT IN WATER

For small amplitude motion of the driven pendulum, no vortex rings are shed as illustrated in Fig. 1(a). As the amplitude of oscillation increases, the pendulum bob begins to shed vortex rings as it reverses direction at the top of each swing. This is shown in Fig. 1(b), where for a continuously driven pendulum, vortex rings stack up as they migrate toward the tank boundaries. Figure 2 shows a time sequence of images depicting the shedding of the boundary layer from the pendulum bob during a directional reversal.

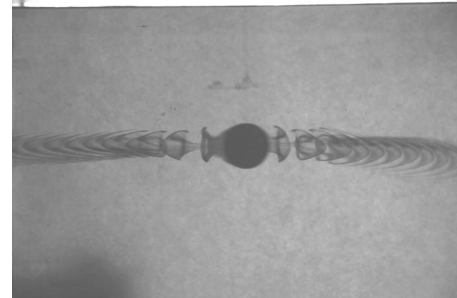
A commonly measured parameter used to quantify the drag force experienced by an object is the dimensionless drag coefficient C_D , defined as

$$C_D = \frac{F}{\frac{1}{2}\rho V^2 A}, \quad (5)$$

where $V = \omega A$ is taken as the characteristic velocity for a given swing, A is the projected area of the sphere, πR_s^2 , and F is the average force over one period. Our photographs allowed us to determine the height y of the sphere above the lowest point at the center of the arc as well as the amplitude A . The change in potential energy ΔU can be easily related to



(a)



(b)

FIG. 1. Photographs of (a) laminar flow at small amplitude oscillation and (b) a street of vortex rings at larger amplitude oscillation.

the work done if the change in height Δy is small, $\Delta U = Mg\Delta y$, where M is the physical mass corrected for buoyancy and g is acceleration due to gravity. The distance traveled during one period is approximately $4A$, so the average work done is $4AF$ and by conservation of energy

$$F = \frac{\Delta U}{4A}. \quad (6)$$

The resulting drag coefficient is shown in Fig. 3. Pixel resolution limits this technique below $Re=300$.

IV. DRAG COEFFICIENT IN LIQUID HELIUM

Schoepe's group at Regensburg produced several pioneering papers on the motion of a small sphere of magnetic material $\sim 100 \mu\text{m}$ in radius, suspended between the superconducting plates of a capacitor, and carrying an electric charge (e.g., [21]). The velocity amplitude and resonance frequency are measured as a function of driving force and temperature in liquid helium at temperatures between 0.35 and 2.2 K. Liquid helium is a Navier-Stokes fluid above 2.176 K and we show their results at 2.2 K in Fig. 3. We also show results at 2.1 K, which can be considered a mixture of normal and superfluid, with the normal-fluid density about 75% of the total density and behaves not far from being a classical fluid. The results are plotted in Fig. 3 and fit with our data remarkably well, especially at higher Reynolds numbers. The effective kinematic viscosity of liquid helium at 2.1 K is about $1.67 \times 10^{-4} \text{ cm}^2/\text{s}$ (Stalp *et al.* [22]) with a Stokes number $St=642$. For our pendulum in water, $St=653$.

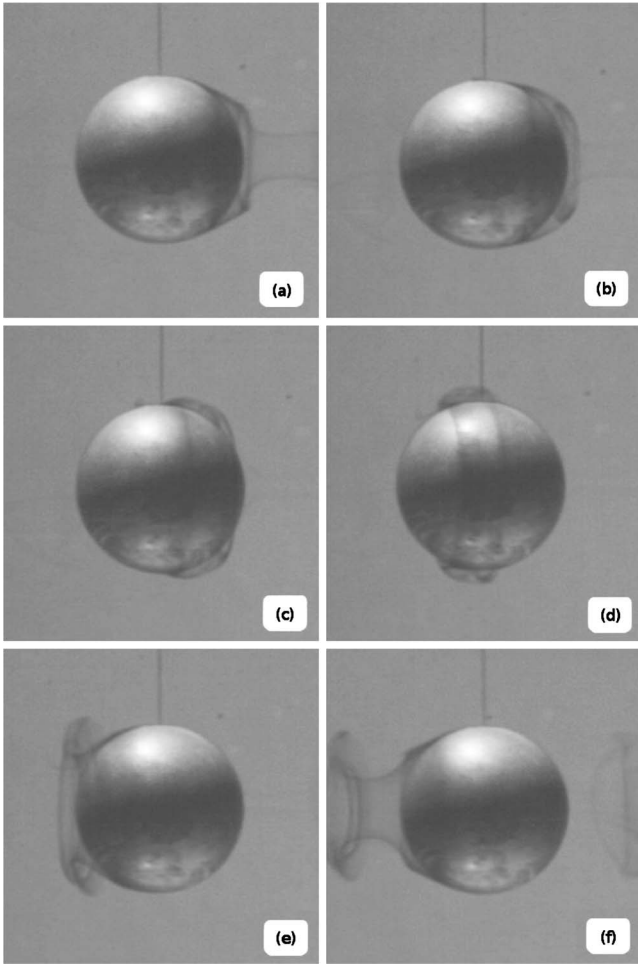


FIG. 2. Time sequence showing the shedding of a vortex ring. Image (a) shows the bob accelerating toward the right.

V. DRAG COEFFICIENT FROM VORTEX RING EMISSION

There is another interesting and useful way to look at the decay data. Figure 4(a) shows a representative sample plot for the amplitude against time for one of the pendulum decays. The plots for the other experimental runs are similar. A

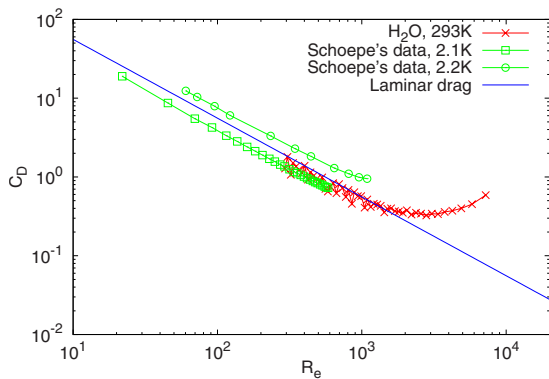


FIG. 3. (Color online) Drag coefficient as a function of Reynolds number, $Re=2R_s\omega A/\nu$. The solid line is the result of Eqs. (1) and (5)

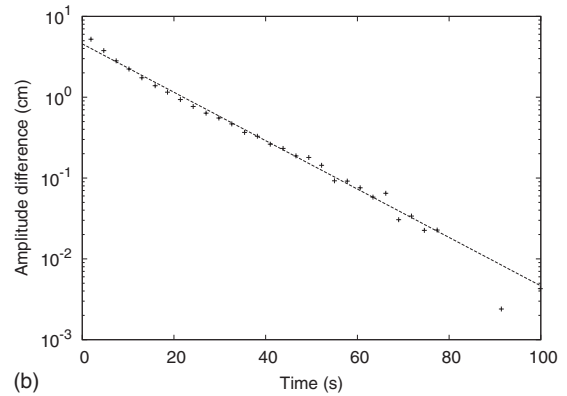
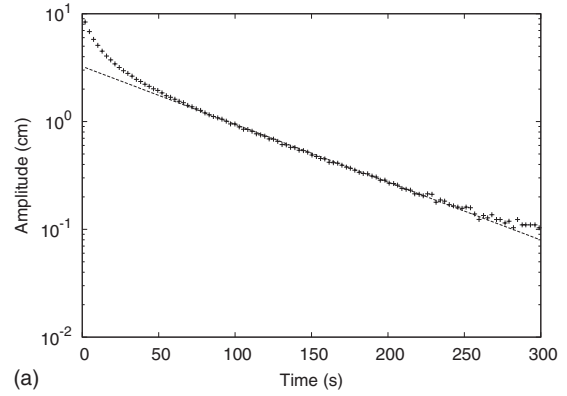


FIG. 4. (a) Amplitude decay of a 5.08 cm pendulum bob and (b) its deviation from Stokes drag (case 6).

list of the experiments conducted is given in Table I. For smaller amplitudes (approximately given by $KC \leq \frac{\pi}{2}$) at later times, the decay is largely exponential and is well approximated by the Stokes drag given in Eq. (1).

At higher amplitudes (early times), the decay exceeds this purely exponential rate. This behavior has previously been observed by many researchers (e.g., Gonzales and Bol [3]). Often nonlinear damping functions are fit to the curve without much physical insight into this additional drag. Figure 4(b) shows a typical log plot of the difference between the Stokes decay and the measured decay of Fig. 4(a) (i.e., the difference in amplitude between the solid and dashed curves). What is noteworthy here is that this difference also appears to decay exponentially. At early times (large amplitudes), a vortex ring is shed from the bob each time it changes direction (at the local position extremes). At later times, no ring is emitted and the boundary layer (largely the inked region) remains attached to the sphere. The point at which this ejection of vortex rings ceases coincides with the point where the amplitude decay begins to follow the Stokes drag law. Thus, we postulate that the excess loss in amplitude, as illustrated in Fig. 4(b), can be accounted for by the impulse lost to each shed vortex ring.

We can estimate the excess drag owing to vortex ring emission in an elementary way. The characteristic momentum of the pendulum is $M\omega A$, where M is the hydrodynamic mass of the bob. This means that the loss of momentum at each half period is $M\omega\Delta A$. A certain amount of momentum is lost owing to Stokes drag. Assuming the excess beyond the

TABLE I. Properties of the spherical bob pendulums used in this investigation.

Case	R_s (cm)	ρ_s (g/cm ³)	m (g)	M (g)	ω (s ⁻¹)	δ (cm)
1	1.27	8.45	2.29	76.8	1.58	0.113
2	1.91	7.65	5.13	238	1.60	0.113
3	2.54	7.63	9.08	561	1.59	0.112
4	1.27	8.45	1.90	76.8	2.27	0.0939
5	1.91	7.65	4.33	238	2.24	0.0945
6	2.54	7.67	7.66	560	2.24	0.0945

Stokes drag is imparted to the fluid with a characteristic velocity equal to that of the pendulum (i.e., ωA), then the momentum imparted to the ejected fluid is given by $M\omega\Delta A = m\omega A$, where m is the mass of the fluid to which momentum is imparted each half cycle. This conservation of momentum principle also works very well for vortex ring guns (Sullivan *et al.* [23]) This gives

$$\frac{\Delta A}{A} = 2\frac{m}{M}, \quad (7)$$

where the value of m is the mass of the boundary layer of thickness δ during oscillation. Using the flat plate analogy, $\delta = \sqrt{2\nu/\omega}$, and

$$m = 4\pi R_s^2 \delta \rho, \quad (8)$$

the hydrodynamic mass of the bob is

$$M = \frac{4}{3}\pi R_s^3 \left(\rho_s + \frac{\rho}{2} \right). \quad (9)$$

We investigated six different cases. The physical properties are contained in Table I and the corresponding decay constants are contained in Table II.

For sufficiently large amplitudes, the *excess* drag beyond the simple Stokes drag for classical fluids is due to a loss of impulse to the shed vortex rings. This is a discrete, rather than continuous, phenomenon. A good analogy would be that of a bouncing inelastic ball. While the ball will continuously lose momentum due to drag exerted by the surrounding fluid, it will also lose momentum during each inelastic collision with the surface on which it is bouncing.

This phenomenon also explains why for larger amplitude decay models such as that presented by Digilov *et al.* [24] the amplitude decay rate depends on the initial condition. This is because the geometric decay rate per oscillation ΔA is proportional to A as given by Eq. (7). Of course, at even larger amplitudes one might expect the flow behind the sphere to become more complex, requiring an empirical fit as is done traditionally.

Referring to Fig. 4(b), we see that

$$\Delta A/A = \lambda_s P, \quad (10)$$

where P is the period, and we can compare the calculated and observed values of λ_s from

$$\lambda_s P = \frac{2\alpha m}{M}, \quad (11)$$

where α is a constant of order unity to be derived from experiment. The value α is needed to allow for such effects as we see in Fig. 2, where the boundary layer is not actually spherically symmetrical. Comparison to experiment (see Table III) yields $\alpha = 7.39 \pm 1.24$.

The fact that α is considerably larger than expected suggests that considerably more fluid is being shed into the ring than is given by the boundary layer. Perhaps the roll-up of the boundary layer entrains external fluid, just as the roll-up from a piston gun entrains external fluid (Eq. 2.19 of [23]). Clearly, this problem merits further investigation.

TABLE II. Results from decay experiments for the six cases of Table I. C_D comes from λ_f . Since λ_s comes from a difference in amplitude, a drag coefficient has no simple meaning. KC_c and Re are the Keuligan-Carpenter and Reynolds numbers at critical amplitude.

Case	λ_f (s ⁻¹)	λ_s (s ⁻¹)	KC_c	St	Re	C_D
1	0.0240 ± 0.0002	0.1153 ± 0.0040	2.69	162	436	0.847
2	0.0136 ± 0.0005	0.0665 ± 0.0044	1.78	371	666	0.654
3	0.0115 ± 0.0003	0.0630 ± 0.0030	1.34	653	876	0.738
4	0.0225 ± 0.0012	0.1020 ± 0.0076	2.24	233	524	0.670
5	0.0176 ± 0.0005	0.1001 ± 0.0052	1.50	521	782	0.714
6	0.0135 ± 0.004	0.0928 ± 0.0037	1.13	919	1040	0.731

TABLE III. Geometric decay of excess drag.

Case	$\Delta A / A$	$2am / M$
1	0.458	0.440
2	0.261	0.319
3	0.249	0.239
4	0.283	0.365
5	0.280	0.269
6	0.260	0.202

VI. VORTEX RING RADIUS AS A FUNCTION OF AMPLITUDE

The radius of the ejected rings grows with the amplitude of swing. We can account for this variation as follows. The impulse of a ring of radius R is $\rho\pi R^2\Gamma$. This must be equal to the momentum in the boundary layer

$$m\omega A = \rho\Gamma\pi R^2. \quad (12)$$

In the spirit of the slug model, we assume the circulation must have the form $\Gamma \propto R_s^2 f$, so the mass of fluid in the boundary layer is given by Eq. (8). Thus,

$$R^2 = \beta\sqrt{A}\delta, \quad (13)$$

where β is a constant of order unity to be derived from experiment. The results are shown in Table IV.

VII. CRITICAL AMPLITUDE FOR VORTEX RING EMISSION

The critical amplitude A_c must be sufficiently large to support a viable vortex ring. The core size a of such a ring in this experiment must be of order δ . The smallest vortex ring will be given by this largest value of the ‘‘slenderness ratio’’ $\epsilon = a/R$. Direct numerical simulation by Archer *et al.* [25] suggested $\epsilon = 0.37$ is the largest value beyond which vorticity from the core will begin to leak out of the bubble. Thus, we estimate that the smallest value of R will be of order $\delta/0.37$. Then,

$$A_c = \frac{R^2 f}{4\omega\delta} = \frac{R^2}{8\pi\delta}. \quad (14)$$

TABLE IV. Comparison of Eq. (2) to experiment. The value of β is determined to be 2.96 ± 0.44 .

A	$0.306\sqrt{A}$	R_{exp}	β
0.945	0.297	0.660	2.22
1.219	0.338	0.805	2.38
1.440	0.367	0.985	2.68
1.619	0.389	1.09	2.80
1.787	0.409	1.32	3.23
2.115	0.445	1.41	3.17
2.392	0.473	1.69	3.57
2.607	0.494	1.67	3.38
2.638	2.58	1.65	3.20

TABLE V. Experimental determination of γ ($\gamma = 7.53 \pm 2.46$).

Case	A_c	$\gamma A_c / \delta$
1	0.786	6.96
2	0.618	5.52
3	1.161	10.4
4	0.347	3.70
5	0.778	8.23
6	0.980	10.4

Since there are uncertainties in all these estimates, we simply write

$$A_c \approx \gamma\delta \quad (15)$$

and determine γ from experiment. We attempt to determine A_c by using plots such as Fig. 4(b). If we take the time at which the amplitude difference falls to some arbitrary minimum (10^{-2} cm in our analysis) and use that time to identify A_c from the plots such as Fig. 4(a), we find from Table V, $\gamma = 7.53 \pm 2.46$ [26]. Thus,

$$A_c \approx 7.53 \sqrt{\frac{2\nu}{\omega}}. \quad (16)$$

Note that the critical velocities observed by Schoepe’s group in helium II are not accounted for by Eq. (16). The results at 2.2 K are in helium I, where $\nu = 1.80 \times 10^{-4}$ cm²/s and $A_c = 3.34 \times 10^{-3}$ cm with corresponding velocity 6.1 cm/s. According to Eq. (16), the three highest points in Reynolds number should start to show a break, which they do. It is gratifying to find that Eq. (16) holds over such a large range of scales. The ratio of the radius of our 2-inch bob to the radius of Schoepe’s microsphere is a factor of 276 and the ratio of the masses of the spheres is 37 million.

VIII. DISCUSSION AND CONCLUSION

We conducted a series of controlled experiments where we measured the decay of a pendulum in water (subject to fluid drag). With these data, we measured the drag coefficient over a range of Reynolds numbers. These measurements compared very favorably to those of [21], who measured the drag on a 100 μ m sphere in liquid helium. This illustrates the true scaling behavior of such a system.

As expected, at smaller amplitudes, the classical Stokes drag theory works well at describing the decay. For larger amplitudes where this does not hold, we have identified a *discrete* drag mechanism, where the pendulum loses momentum by shedding vortex rings at the maximum amplitudes while reversing its direction motion. We can estimate the momentum lost to each of these rings by assuming that the mass of fluid in the boundary layer surrounding the sphere, of thickness δ , has the same characteristic velocity as the bob. To the best of our knowledge, this *discrete* mechanism has not previously been identified and only complicated non-

linear fitting curves have been used to attempt to model it.

The relatively large scatter in the experimentally determined quantities α , β , and γ is, in part, the consequence of using such a simple apparatus. For example, when vortex rings are ejected, the pendulum is buffeted and only the 2-inch pendulum was massive enough to persist in its path to measure the drag coefficient in decay. We know from experience that even vortex rings generated in a careful experiment by a piston have substantial scatter in velocity and decay owing to the growth of bending waves on the core, which are very difficult to control (see Fig. 12 in [25]).

There are other limitations to our analysis. The boundary layer on the sphere is not uniform. The vortex rings are not isolated. The rings are close enough to interact with each other and the bob. Further, the errors in the critical amplitude we measure come about because the amplitude at which ring shedding stops in an experiment does not necessarily coin-

cide exactly with the critical amplitude. The amplitudes reached by the pendulum are discrete rather than continuous numbers (i.e., the amplitude at which ejection stops is the first amplitude less than or equal to the critical one). This may also induce errors in the vortex ring radius predictions. Nevertheless, we believe much insight is gained from this simple experiment and we know of no results in the literature for the onset of discrete vortex emission which have the predictive power of Eq. (15).

ACKNOWLEDGMENTS

We thank Wilfried Schoepe for reading the paper and suggesting changes, as well as supplying his unpublished data at 2.2 K. Joe Vinen encouraged us to do this investigation and helped clarify a number of points.

-
- [1] G. Stokes, *Trans. Cambridge Philos. Soc.* **9**, 8 (1858).
 - [2] L. D. Landau and E. M. Lifshitz, *Fluid Mechanics*, 1st ed. (Pergamon, London, 1959).
 - [3] M. I. Gonzalez and A. Bol, *Eur. J. Phys.* **27**, 257 (2006).
 - [4] P. Alexander and E. Indelicato, *Eur. J. Phys.* **26**, 1 (2005).
 - [5] J. Mordant and J.-F. Pinton, *Eur. Phys. J. B* **18**, 343 (2000).
 - [6] N. Lyotard, W. L. Shew, L. Bocquet, and J.-F. Pinton, *Eur. Phys. J. B* **60**, 469 (2007).
 - [7] L. Skrbek and W. F. Vinen, *Progress in Low Temperature Physics XVI* (Elsevier, Amsterdam, 2009), Chap. 4.
 - [8] P. F. Linden and J. S. Turner, *Proc. R. Soc. London, Ser. B* **271**, 647 (2004).
 - [9] J. O. Dabiri and M. Gharib, *Proc. R. Soc. London, Ser. B* **272**, 1557 (2005).
 - [10] K. D. von Ellenrieder, K. Parker, and J. Soria, *Exp. Therm. Fluid Sci.* **32**, 1578 (2008).
 - [11] P. Blondeaux, F. Fornarelli, L. Guglielmini, M. S. Traintafyllou, and R. Verzicco, *Phys. Fluids* **17**, 113601 (2005).
 - [12] Y. Afanasyev, *Phys. Fluids* **17**, 038104 (2005).
 - [13] S. Taneda, *J. Phys. Soc. Jpn.* **11**, 1104 (1956).
 - [14] M. Bentwich and T. Miloh, *J. Fluid Mech.* **88**, 17 (1978).
 - [15] T. Sano, *J. Fluid Mech.* **112**, 433 (1981).
 - [16] B. U. Felderhof, *Phys. Fluids* **19**, 073102 (2007).
 - [17] G. Yun, D. Kim, and H. Choi, *Phys. Fluids* **18**, 015102 (2006).
 - [18] H. M. Blackburn, *Phys. Fluids* **14**, 3983 (2002).
 - [19] G. Constantinescu and K. Squires, *Phys. Fluids* **16**, 1449 (2004).
 - [20] R. M. Mazo, R. Hershberger, and R. J. Donnelly, *Exp. Fluids* **44**, 49 (2008).
 - [21] J. Jäger, B. Schuderer, and W. Schoepe, *Physica B* **210**, 201 (1995).
 - [22] S. R. Stalp, J. J. Niemela, W. F. Vinen, and R. J. Donnelly, *Phys. Fluids* **14**, 1377 (2002).
 - [23] I. S. Sullivan, J. J. Niemela, R. E. Hershberger, D. Bolster, and R. J. Donnelly, *J. Fluid Mech.* **609**, 319 (2008).
 - [24] R. Digilov, M. Reiner, and Z. Weizman, *Am. J. Phys.* **73**, 901 (2005).
 - [25] P. J. Archer, T. G. Thomas, and G. N. Coleman, *J. Fluid Mech.* **598**, 201 (2008).
 - [26] Case 4 of Table V looks like an outlier: it was the least massive ball and the shortest pendulum and therefore the fewest swings. If case 4 were omitted, we would have $\beta = 8.29 \pm 1.93$, a considerably lower uncertainty.